

# Elevated citrate in pediatric astrocytomas with malignant progression

Stefan Blüml, Ashok Panigrahy, Mikhail Laskov, Girish Dhall, Mark D. Krieger, Marvin D. Nelson, Jonathan L. Finlay, and Floyd H. Gilles

Department of Radiology (S.B., A.P., M.D.N.), Division of Neurosurgery (M.D.K.), Children's Center for Cancer and Blood Diseases (M.L., G.D., J.L.F.), Department of Neuropathology, Children's Hospital-Los Angeles, Los Angeles, CA, USA (F.H.G.); Rudi Schulte Research Institute, Santa Barbara, CA, USA (S.B.)

In vivo magnetic resonance spectroscopy (MRS) provides information about metabolite concentrations in tissue. Recently citrate was detected by MRS in subgroups of pediatric brain tumors. Citrate is an intermediate in the tricarboxylic acid (TCA) cycle and accumulates in tissue when the glycolytic rate exceeds the TCA cycle activity, a feature of malignant tumors. Currently, no practical indicators allow clinicians to predict risk for malignant progression of pediatric astrocytomas (World Health Organization [WHO] grade II). Medical records and citrate concentrations measured with in vivo MRS of 29 pediatric astrocytomas were reviewed. This included 6 patients with astrocytomas (WHO II) who had stable disease (indolent LGA) for >2 years, 7 with aggressive grade II astrocytomas (aggressive LGA), 13 with anaplastic astrocytomas (WHO III), and 3 with glioblastoma (WHO IV) with disease progression within 2 years. Citrate was observed in all patients with aggressive LGA, and the mean citrate concentration was significantly higher in this group than among those with indolent LGA (mean  $\pm$  standard deviation,  $4.1 \pm 1.1$  vs  $0.6 \pm 0.8$  mmol/kg;  $P < .0001$ ). There was no consistent pattern for citrate in anaplastic astrocytoma and glioblastoma, with citrate prominent in some lesions whereas undetectable in others. It is unclear whether citrate accumulation occurred because of fundamental defects of citrate regulation or was secondary to altered physiological conditions. Nonetheless, prominent citrate identified a subgroup of pediatric grade II astrocytomas destined for aggressive behavior. Citrate

was not specific for poor outcome because it was not detectable in all high-grade astrocytomas. In high-grade astrocytoma, tumors with prominent citrate may constitute a metabolic subclass.

**Keywords:** astrocytoma, citrate, metabolism, MR spectroscopy, pediatrics.

In vivo magnetic resonance spectroscopy (MRS) provides information about the biochemistry of tissue by assessing concentrations or relative concentrations of metabolites and other small low-weight molecules. A recently reported chemical detectable in subgroups of pediatric brain tumors is citrate.<sup>1</sup> Citrate is an intermediate in the tricarboxylic acid (TCA) cycle and accumulates in tissue where the glycolytic rate exceeds the TCA cycle activity, a long-known feature of malignant tumors.<sup>2,3</sup> Excessive citrate can be used by cells to transport mitochondrial acetyl-CoA carbons to the cytoplasm for the biosynthesis of fatty acids ultimately needed for the de novo synthesis of cell membranes. This is an essential step to support cell divisions and to increase the production of biomass of growing tumors.<sup>4</sup> In vivo citrate levels were reported to be particularly high in pontine gliomas<sup>1</sup>—tumors with apparently inevitable aggressive behavior, despite presenting frequently with histopathological features typical for grade II diffuse astrocytomas.<sup>5–11</sup>

The overall objective of this retrospective study was to examine the significance of citrate accumulation in pediatric astrocytomas outside the pons. Specifically, the goals were (1) to determine whether high citrate levels separated aggressive from indolent grade II astrocytoma, (2) to examine whether prominent citrate was a specific feature of tumors with poor outcome also observed in high-grade astrocytomas, and (3) to determine whether citrate accumulation correlated with magnetic resonance radiographic features of the lesions.

Received November 2, 2010; accepted May 13, 2011.

Corresponding Author: Stefan Blüml, PhD, Department of Radiology, Children's Hospital Los Angeles, MS 81, 4650 Sunset Boulevard, Los Angeles, CA 90027, USA (sbluml@chla.usc.edu).  
Current affiliation: Department of Pediatric Radiology, Children's Hospital of Pittsburgh of UPMC, Pittsburgh, PA, USA (A.P.); Pediatric Oncology Department, N.N. Blokhin Russian Cancer Research Center, Moscow, Russia (M.L.).

## Material and Methods

### Patients

Pediatric patients with biopsy-confirmed astrocytoma who underwent MRS studies were considered for this study. We included only patients who underwent at least 1 MRS study in which the region of interest that was selected for MRS enclosed only tumor tissue without partial volume of surrounding normal appearing tissue as judged by 2 pediatric neuroradiologists. This assessment was performed prior to and independent of the review of clinical information and was extracted from an already existing MRS database. This list of patients (40 subjects) was distributed to the clinicians for a review of the medical records. Subsequent to the review, 9 patients with <2 years of clinical follow-up, unless they died of complications due to progressive disease within that period, were excluded. Also excluded were 2 patients who died of other causes, such as sepsis or organ failure.

Results of only 1 MRS study per patient were analyzed. This was, when available, the MRS study obtained at the time of initial diagnosis. Otherwise, the study closest to initial diagnosis was selected. All pathological assignments were based on initial biopsy findings, and consensus was reached for each tumor. Six patients were identified with diffuse low-grade astrocytoma (World Health Organization [WHO] grade II) and no clinical and radiological progression over  $\geq 2$  years of follow-up (indolent LGA). Seven patients were identified with diffuse low-grade astrocytoma (WHO grade II) with progression  $\leq 2$  years after diagnosis (aggressive LGA). We also analyzed data obtained from 13 children with anaplastic astrocytoma (AA; WHO grade III) and 3 pediatric patients with glioblastoma (GBM; WHO grade IV) with progression in  $\leq 2$  years. All patients with indolent LGA were alive, whereas all with aggressive LGA, AA, and GBM had died of their disease by the time of the completion of this study. Clinical information reviewed for each subject included the time of diagnosis, time to disease progression and death, treatments received, pathology, and surgical reports, as well as the time of MRS studies relative to the time of diagnoses and therapies (Table 1). Criteria for disease progression were new or worsening clinical symptoms, such as problems with swallowing, speech, and walking, during a clinical consultation. In cases in which there were any doubts about disease progression based on these clinical symptoms alone, clinicians ordered a magnetic resonance study, which confirmed a significant growth of a lesion (as per the Children's Oncology Group guidelines: "20% or more increase in the product of perpendicular diameters of ANY target lesion, or the appearance of one or more new lesions."<sup>12</sup>). Progression was also diagnosed when a significant worsening of the disease was noted on MRI and subsequently confirmed by a clinical evaluation (criteria as above). The selection of patients and sorting them into indolent LGA, aggressive LGA, AA, and GBM was performed by 2

authors (M.L. and J.L.F.) and was independent of the fully automated MRS data analysis (this is explained in detail below).

This retrospective study was approved by the Institutional Review Board (IRB). Some of the patients were previously enrolled in prospective research studies and parental consent was obtained. For other patients, MRS data were obtained as part of routine clinical evaluations. For these cases, the IRB permitted the review of already existing data and medical records, and the requirement for parental consent was waived.

### MRS Acquisition and Quantitation

All MRS studies were performed on a 1.5T MR system (Signa LX; GE Healthcare). Patients aged  $\leq 5$  years were anesthetized with 100–200  $\mu\text{g}/\text{min}/\text{kg}$  propofol throughout the magnetic resonance study. Single-voxel point-resolved spectroscopy (PRESS) with a short echo time of  $\text{TE} = 35$  ms, a repetition time of  $\text{TR} = 1.5$  s, and 128 signal averages was used for all acquisitions. With these parameters, the total acquisition time, including scanner adjustments, was less than 5 minutes. All MRS data were acquired prior to contrast injection (Magnevist [gadopentetate dimeglumine], Bayer Healthcare). T2-weighted fast spin-echo, FLAIR, and T1-weighted FLAIR images were acquired in all cases before contrast injection and reviewed to determine the extension of a lesion. The position of the region of interest selected for MRS was documented on 3 MRIs and reviewed to ensure that no partial volume for normal appearing tissue was enclosed. Sizes and shapes of the regions of interest were adjusted to the lesion sizes and typically varied from 5 to 10  $\text{cm}^3$ . Spectra were processed using fully automated LCModel software (Stephen Provencher, Canada, LCModel Version 6.1-4F), and absolute metabolite concentrations (in  $\text{mmol}/\text{kg}$  tissue) of citrate were determined. Also measured were the concentrations of N-acetylaspartate (NAA), creatine, total choline, myo-inositol, glutamate, glutamine, the sum of Glu and Gln (Glx), guanidinoacetate, and lactate, as well as lipid (and possibly underlying macromolecules) intensities at 0.9 ppm (parts per million) and 1.3 ppm (LipMM09 and LipMM13), as described in detail in previous publications.<sup>13–15</sup> Often relative concentration ratios instead of absolute concentrations are reported in the literature. To allow comparisons with these studies, we also analyzed concentration ratios relative to creatine level.

### Radiographic Appearance

The anatomical location and the contrast enhancement pattern of the lesions were reviewed to determine whether citrate accumulation was limited to tumors in certain brain regions or to tumors with intact/impaired blood-brain-barrier. The apparent diffusion coefficient (ADC), a quantitative measure of the diffusion of water molecules within tissue, was also analyzed. To measure ADC, an echo-planar sequence with an echo time TE of 85 ms, 5–7 mm slice thickness, 20–26 cm field of view, 128  $\times$  128 matrix size, and a b-value of

**Table 1.** Summary of patients' demographic characteristics

Age at diagnosis, years	Sex	Lesion appearance/location	Time of MRS scan	Treatments prior to MRS	Time without/ to progression, months <sup>a</sup>	Remarks
Grade II diffuse astrocytoma with stable disease						
11.2	M	Nonenhancing thalamic tumor	25 months after Dx	RT + TEM	>60	
6.4	F	Cerebellar non-enhancing lesion	At initial presentation	None	>49	
4.5	F	Infiltrating non-enhancing bithalamic lesion with involvement of brainstem	3 months after Dx, post biopsy	None	>41	See Fig. 2
17.8	F	Minimally enhancing pineal region mass	5 years after Dx	RT	>60	
13.3	M	Nonenhancing tectal plate glioma	6 months after Dx	None	>30	
1.1	M	Minimally enhancing intraventricular mass	At initial presentation	None	>24	
10.3 ± 6.5	3M/3F				>44 ± 15	
Grade II diffuse astrocytoma with aggressive behavior						
4.1	M	Heterogeneous enhancing, hemorrhagic right frontal mass	At initial presentation	None	24	Recurrent as grade III after 2 yrs
13.3	F	Frontal lobe cystic/enhancing lesion	15 months after Dx, increased symptoms	Chemotherapy	8	
5.0	F	Bithalamic nonenhancing mass	At initial presentation	None	5	See Fig. 3
8.4	F	Nonenhancing tectal plate glioma	6 months after Dx, post biopsy	None/observation	18	Recurrent as grade III after 18 months
13.6	M	Patchy enhancing and infiltrating mass at posterior thalamus	11 months after Dx, increased symptoms	Shunt/observation	10	
6.0	F	Both enhancing and non-enhancing splenium/callosal lesion	3 months after Dx, increased symptoms	Partial resection/observation	0	Progressed to grade IV
7.8	F	Heterogeneous mass with solid cystic components at left cerebellar peduncle and brainstem	12 months after Dx, recurrent disease	Partial resection/observation	18	
8.3 ± 3.8	2 M/5 F				11.9 ± 8.5	
Anaplastic astrocytoma (WHO III)						
8.1	M	Cystic/solid enhancing bifrontal mass with extensive edema	3 months post Dx, residual tumor	partial resection, RT + IRI + TEM	7	
6.1	F	Mildly enhancing thalamic lesion	At initial presentation	None	17	
18.7	F	Minimal enhancing frontal mass	At initial presentation	None	8	
6.9	M	Nonenhancing enlargement of thalamus	At initial presentation	None	8	Glimatosis cerebri; see Fig. 4A
14.3	F	Bithalamic tumor with heterogeneous enhancement	3 months after Dx	TEM	4	
17.9	F	Extensive lesion with enhancing areas	2 months after Dx, Post-biopsy	TEM (four days)	1	Glimatosis cerebri
14.2	M	Temporal lobe lesion with focal areas of enhancement	At initial presentation	None	7	Glimatosis cerebri
15.6	M	Nodular enhancing lesion at fourth ventricle	2 months after Dx	RT (spine) + TEM <sup>b</sup>	1	History of spinal cord AA
16.0	M	Non-enhancing thalamic tumor with intraventricular extension	At initial presentation	None	10	

*Continued*

Table 1. Continued

Age at diagnosis, years	Sex	Lesion appearance/location	Time of MRS scan	Treatments prior to MRS	Time without/ to progression, months <sup>a</sup>	Remarks
6.1	M	Nonenhancing parieto-occipital mass	At initial presentation	RT (spine) + TEM <sup>b</sup>	5	History of spinal cord AA
7.4	F	Mildly-enhancing thalamic tumor with intraventricular extension	At initial presentation	None	4	Highest citrate, very bright lesion (see Fig. 4B)
4.4	F	Minimally enhancing bithalamic lesion	2 months after Dx	Shunt, TEM	22	
8.5	M	Enhancing necrotic mass in posterior basal ganglia	1 month after Dx	Partial resection	1	
11.1 ± 5.1	7M/6F				7.3 ± 6.2	
Glioblastoma (WHO IV)						
5.2	M	Heterogeneously enhancing mass at right brainstem	At initial presentation	None	3	
14.7	M	Necrotic/enhancing temporal lobe mass	1 month after Dx	Partial resection	1	
4.1	F	Multilobulated heterogeneously enhancing solid/cystic left parietal mass	3 months after Dx	Partial resection, chemotherapy	2	
8.0 ± 5.8	2 M/1 F				2.0 ± 1.0	

Dx indicates diagnosis; IRI indicates irinotecan; RT indicates radiation therapy; TEM indicates temozolomide.

<sup>a</sup>Indicates the minimum time of progression-free survival of stable LGA and the time to progression for all other patients after initial diagnoses.

<sup>b</sup>Treatments of the spinal cord tumors.

1000 s/mm<sup>2</sup> was used. The magnetic resonance diffusion scans were conducted before contrast agents were administered. Manufacturer-provided software was used to calculate ADC maps. The maps were then stored on the hospital PACS system (Synapse; Fuji), and the mean ADCs for regions that matched areas selected for the MRS studies were computed.

### Statistical Analyses

As the primary goal of this study was to specifically test whether citrate was different in aggressive and indolent low-grade astrocytomas, an unpaired 2-tailed Student's *t*-test with unequal variance was considered to be the appropriate method. The Student's *t*-test was also used to test for other metabolic features that might be different in these 2 groups. The Cramer-Rao lower bounds (CRLBs) were used to determine whether there was evidence of the presence of citrate in spectra of high-grade astrocytomas. CRLBs are objective indicators for the reliability of fit, taking into consideration the noise level of the magnetic resonance signal. A CRLB of >100% indicated that there was no evidence of citrate in the spectrum. To determine whether citrate levels correlated with the ADC, data from all patients were pooled, and the Pearson correlation coefficient was calculated.

## Results

### Citrate Levels in Aggressive and Indolent Grade II Astrocytomas

Citrate was significantly higher in grade II astrocytoma with disease progression in ≤2 years than in stable grade II astrocytoma (mean ± standard deviation, 4.1 ± 1.1 vs 0.6 ± 0.8 mmol/kg; *P* < .0001, by Student *t* test). The concentration ratio of citrate relative to creatine was also significantly higher in aggressive LGA versus indolent LGA (0.7 ± 0.3 vs 0.1 ± 0.1; *P* < .001) (Figs 1–3). In addition, NAA was significantly reduced in aggressive LGA versus indolent LGA, but at a lower level of significance (0.7 ± 0.7 vs. 2.9 ± 1.1 mmol/kg; *P* < .01). No other metabolic features were significantly different (Table 2).

### Citrate in High-grade Astrocytomas

Prominent citrate was *not* a specific feature of high-grade astrocytomas with poor outcome (Fig. 4). In anaplastic astrocytomas, citrate levels varied considerably in individual patients (2.7 ± 2.7 mmol/kg; range, 0.0–10.1 mmol/kg). The tumor with highest level of citrate included in this study was in a patient with anaplastic astrocytoma. However, citrate was undetectable in 3 patients with anaplastic astrocytomas. Data from only 3 patients with GBM at diagnosis were available for this study. The averaged spectrum from these patients showed no evidence for citrate (Fig. 5).

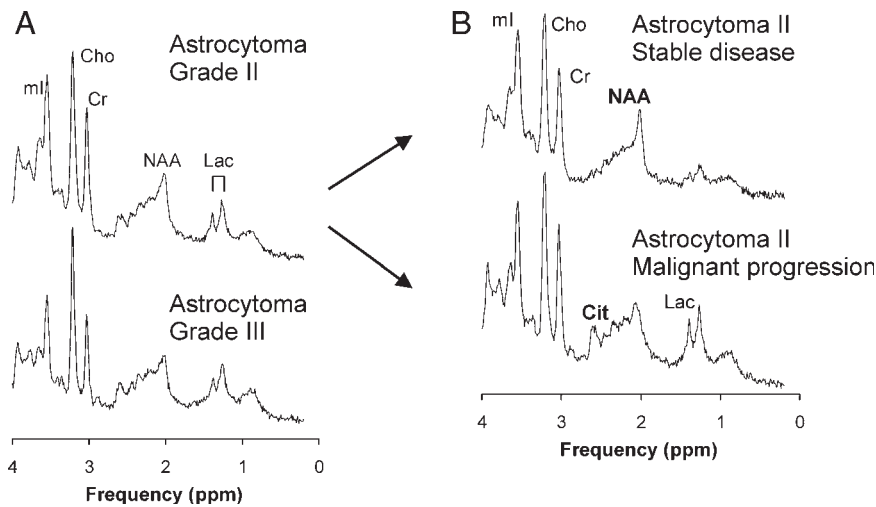


Fig. 1. Shown are averaged spectra computed from all grade II astrocytoma and of all grade III astrocytoma. Overall, the patterns were comparable (A). When grade II astrocytomas were subdivided into 2 groups according to clinical outcome, citrate (Cit) at ~2.6 ppm was significantly more prominent in aggressive astrocytoma (B). Other chemicals that can be quantified with in vivo MR spectroscopy include N-acetyl-aspartate (NAA), creatine (Cr), lactate (Lac), choline (Cho), and myo-inositol (ml). Note that NAA levels in aggressive astrocytoma were significantly lower than in stable astrocytoma but to a much lesser extent than citrate. Despite the more prominent appearance of lactate in grade II astrocytomas with malignant progression, significance was not reached due to considerable scatter of measured concentrations. All spectra are scaled to the measured concentrations to allow direct comparison.

#### Correlation of Citrate Accumulation with Radiographic Appearance

When all data from all patients were pooled, there was a weak but significant positive correlation between citrate level and the tissue ADC ( $r^2 = 0.6$ ;  $P < .001$ , by Pearson correlation). Citrate accumulated in enhancing and nonenhancing lesions, and there was no apparent correlation with lesion location (Table 1).

#### Other Metabolic Features of Pediatric Astrocytomas

All metabolite concentrations and ratios measured with our MRS method for indolent LGA, aggressive LGA, and AA are summarized in Table 2. These metabolic features were analyzed using analysis of variance and the Fisher multiple comparison test. The analyses did not reveal any significant additional findings and are thus not described in detail. In addition, when indolent LGA and aggressive LGA were pooled and compared with anaplastic astrocytoma, there were no significant differences observed. Some of the differences between low-grade and high-grade astrocytomas reported in the literature,<sup>16–18</sup> such as generally higher mean total choline, lactate, and lipid levels in high-grade astrocytomas, were observed but did not reach significance.

## Discussion

#### Prominent Citrate in Aggressive LGA

Citrate is a key metabolite in the TCA cycle and can accumulate in tissues with increased glycolytic rates in the absence of equally up-regulated TCA cycle activity,

a well-known feature of malignant tumors (ie, the Warburg effect). Our study identified prominent citrate as a metabolic feature that distinguished aggressive pediatric astrocytomas from stable astrocytoma. This included patients for whom MRS was performed *before* clinical or radiological manifestation of aggressive disease. Previously, it was reported that citrate was abnormally elevated in pontine gliomas.<sup>1</sup> For these tumors, the detection of citrate at diagnosis adds little to the already poor prognosis. On the other hand, stratification of astrocytomas outside the pons is a significant problem in pediatric neuro-oncology, and early identification of astrocytomas that are destined for malignant progression has a significant impact on patient management.

For each patient, we analyzed only 1 MRS study performed at the time of diagnosis or close to diagnosis. This avoided emphasizing results from individual more frequently examined patients. Additional analyses (not reported in detail) showed that pooling all studies or analyzing only the latest available study for each patient would not alter any of the reported findings.

#### Variability of Citrate in AA and Glioblastomas

Prominent citrate was *not* a specific feature of tumors with poor prognoses. Indeed, among the 13 patients with AA included in this study, there was no evidence for citrate in three patients. On the other hand, of all patients, the tumor with the highest citrate concentration was among those with AA. Because all of the MRS studies of AA were performed at initial diagnosis or within the first 3 months after diagnosis, it is unlikely that the timing of the study had an impact on this finding. A more likely scenario is that the considerable



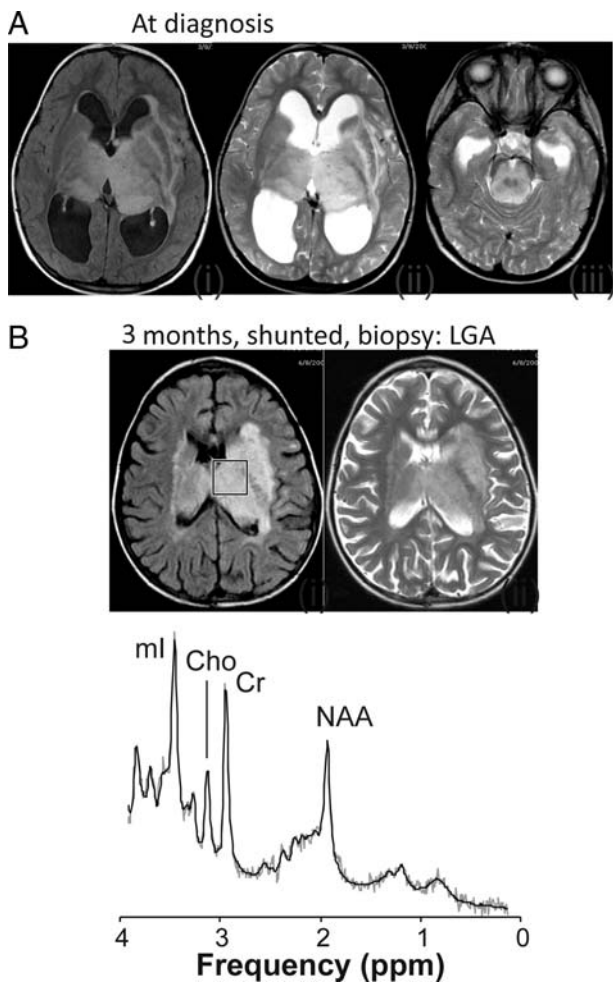


Fig. 2. Transverse fluid-attenuated inversion recovery (FLAIR) and T2-weighted magnetic resonance image (MRI) for a patient with an infiltrating nonenhancing bithalamic lesion extending into parts of the brainstem with enlarged ventricles and periventricular edema at diagnosis (A). A magnetic resonance spectrum was not obtained at diagnosis. The patient subsequently underwent shunt surgery, and a biopsy of the lesion was performed (grade II diffuse astrocytoma). MRI at three months demonstrated reduced size of the ventricles and resolved edema (B). In the spectrum obtained at that time of the tumor, N-acetyl-aspartate (NAA), creatine (Cr), choline (Cho), and myo-inositol (ml) were readily detectable. There was no evidence for citrate. Shown are the unfiltered raw data (thin grey line) and the fit to the data used for quantitation (black line). The box on the FLAIR MR image (B) indicates the region of interest from where the spectrum was acquired. This patient is alive and doing well 5 years after initial diagnosis.

metabolic heterogeneity of AA is a reflection of histological and genetic subclasses of these tumors.<sup>19–23</sup> Tumors with prominent citrate may constitute a metabolic subclass among AA. The averaged GBM spectrum showed no evidence of the presence of citrate in these tumors. At this stage, this observation cannot be generalized due to the small number of patients with GBM. Nevertheless, it is evident that citrate was not a specific feature of tumors with poor outcome.

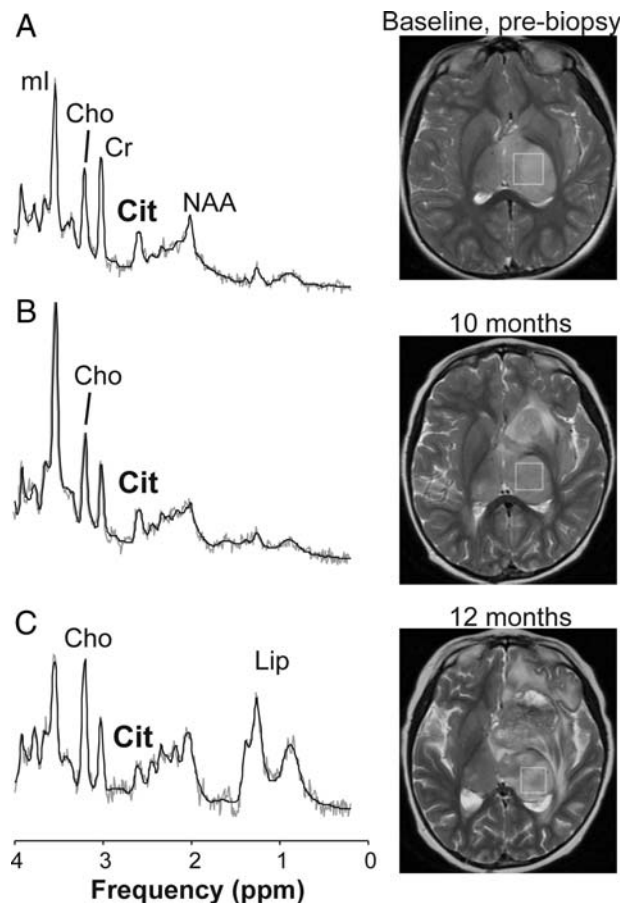


Fig. 3. Magnetic resonance spectra and T2-weighted magnetic resonance image (MRI) indicating the region of interest from which spectra were obtained of a grade II bithalamic astrocytoma with aggressive behavior. A spectrum acquired from a nonenhancing diffuse astrocytoma at initial presentation (A) shows no evidence of elevated lipids or lactate (Lac) and choline (Cho) levels are moderate. On the other hand, citrate (Cit) is readily detectable at baseline (cf. Fig. 2). Progressive disease was apparent on MRI within 1 year after initial diagnosis (B and C), and the patient died within 2 years after diagnosis. Only the spectrum obtained at baseline was used for the analysis of differences between aggressive and indolent grade II astrocytomas. Note that Cho, Lac, and lipid (Lip) levels increased as the disease progressed, whereas the citrate level did not increase but may have decreased slightly in this patient. A similar trend of decreasing citrate levels was reported earlier for progressing diffuse pontine gliomas.<sup>15</sup>

#### Radiographic Features of Astrocytomas with High Citrate Levels

There was no apparent association between citrate levels and contrast enhancement or the location of a tumor. However, there was a positive correlation between citrate concentrations and the ADCs. Because diffusion imaging is sensitive to the extracellular space, this observation indicated a correlation of citrate concentrations with the amount of interstitial fluid and swelling. There is a correlation between ADC and the T2 relaxation time of tissue.<sup>24</sup> This means that tumors with

**Table 2.** Absolute concentrations (mmol/kg tissue) and metabolite concentration ratios relative to creatine level (mean  $\pm$  standard deviation) of pediatric astrocytomas

	All LGA	Indolent disease	Astrocytomas with malignant progression	
		Indolent LGA	Aggressive LGA	AA
N	13	6	7	13
[Cit]	2.5 $\pm$ 2.1	0.6 $\pm$ 0.8	4.1 $\pm$ 1.1***	2.7 $\pm$ 2.7
[NAA]	1.7 $\pm$ 1.4	2.9 $\pm$ 1.1	0.7 $\pm$ 0.7*	1.6 $\pm$ 0.8
[Cr]	7.8 $\pm$ 2.4	8.4 $\pm$ 1.3	7.3 $\pm$ 3.0	6.3 $\pm$ 2.3
[Cho]	3.5 $\pm$ 1.2	3.3 $\pm$ 1.4	3.6 $\pm$ 1.2	3.6 $\pm$ 1.8
[ml]	12.1 $\pm$ 4.9	13.2 $\pm$ 4.6	11.2 $\pm$ 5.7	10.8 $\pm$ 4.6
[Lac] <sup>a</sup>	2.8 $\pm$ 3.6	0.7 $\pm$ 0.6	4.6 $\pm$ 4.1	1.8 $\pm$ 1.3
[Gln]	8.8 $\pm$ 3.8	6.9 $\pm$ 1.7	10.4 $\pm$ 4.5	7.2 $\pm$ 4.7
[Glu]	3.4 $\pm$ 2.7	5.1 $\pm$ 2.2	2.0 $\pm$ 2.3	3.6 $\pm$ 2.3
[Glx] <sup>b</sup>	12.2 $\pm$ 4.2	12.1 $\pm$ 2.1	12.4 $\pm$ 5.7	10.8 $\pm$ 5.2
[Gua]	1.6 $\pm$ 1.2	1.0 $\pm$ 0.9	2.0 $\pm$ 1.4	1.7 $\pm$ 0.4
[Cit]/[Cr]	0.4 $\pm$ 0.4	0.1 $\pm$ 0.1	0.7 $\pm$ 0.3**	0.6 $\pm$ 0.9
[NAA]/[Cr]	0.2 $\pm$ 0.2	0.4 $\pm$ 0.2	0.1 $\pm$ 0.1	0.3 $\pm$ 0.2
[Cho]/[Cr]	0.5 $\pm$ 0.3	0.4 $\pm$ 0.1	0.6 $\pm$ 0.3	0.7 $\pm$ 0.4
[ml]/[Cr]	1.6 $\pm$ 0.5	1.6 $\pm$ 0.5	1.6 $\pm$ 0.5	1.8 $\pm$ 0.5
[Lac]/[Cr]	0.6 $\pm$ 1.0	0.1 $\pm$ 0.1	1.1 $\pm$ 1.2	0.4 $\pm$ 0.4
[Gln]/[Cr]	1.1 $\pm$ 0.8	0.7 $\pm$ 0.1	1.5 $\pm$ 0.9	1.0 $\pm$ 0.7
[Glu]/[Cr]	0.5 $\pm$ 0.4	0.6 $\pm$ 0.3	0.4 $\pm$ 0.4	0.6 $\pm$ 0.4
[Glx]/[Cr]	1.6 $\pm$ 0.9	1.3 $\pm$ 0.3	1.8 $\pm$ 1.2	1.7 $\pm$ 0.8
[Gua]/[Cr]	0.3 $\pm$ 0.2	0.1 $\pm$ 0.1	0.3 $\pm$ 0.3	0.3 $\pm$ 0.2
<sup>c</sup> LipMM09	6.0 $\pm$ 2.5	4.4 $\pm$ 0.8	7.4 $\pm$ 2.6	7.5 $\pm$ 4.4
<sup>c</sup> LipMM13	10.9 $\pm$ 8.5	7.3 $\pm$ 3.0	14.0 $\pm$ 10.6	11.9 $\pm$ 10.6
<sup>d</sup> ADC	1.16 $\pm$ 0.15	1.10 $\pm$ 0.14	1.21 $\pm$ 0.16	1.15 $\pm$ 0.34

For aggressive versus indolent LGA, \* $P < .01$ , \*\* $P < .001$ , and \*\*\* $P < .0001$ .

<sup>a</sup>Lactate concentrations are reported in mmol/L.

<sup>b</sup>[Glx] = [glutamate] + [glutamine].

<sup>c</sup>Absolute intensity (arbitrary units).

<sup>d</sup>In  $\text{mm}^2/\text{s} \times 10^{-3}$ .

higher citrate concentrations were generally brighter on T2-weighted MRIs. The finding of a positive correlation between ADC and citrate may be counterintuitive, because one might expect lesions with higher cellularity (ie, lower ADC) to be more aggressive. However, this observation of an inverse correlation between ADC and aggressiveness was made in adults with glioblastoma<sup>25,26</sup> and may not generally be applicable in pediatrics. For example, pediatric pontine gliomas are characterized by high initial ADC values<sup>27</sup> (and high citrate concentrations<sup>1</sup>), despite having the worst outcomes of all tumors in pediatric neuro-oncology.

#### What Causes Citrate Accumulation?

It is unclear which mechanisms caused increased citrate in some of the tumors. Recently, mutations of the isocitrate dehydrogenase 1 gene (IDH1) have been detected in human gliomas.<sup>28</sup> IDH1 mutations are considered to be early events in the progression of a tumor,<sup>29</sup> preceding other genetic mutations associated with gliomas, and have been linked with upregulation of processes (eg, angiogenesis) that promote tumor growth.<sup>23,30,31</sup> Although the exact impact of IDH1

mutations is unclear, there is evidence that they can cause an inhibition of the catalysis of isocitrate to  $\alpha$ -ketoglutarate.<sup>32</sup> Because the conversion of citrate to isocitrate is reversible, citrate may potentially accumulate in tissue with impaired IDH1 activity. IDH1 mutations were most frequently observed in secondary GBM (73%–88%),<sup>21</sup> evolving from low-grade astrocytomas. IDH1 mutations were also frequently observed in grade II diffuse astrocytoma (59%–88%), and anaplastic astrocytoma (50%–78%), whereas there is a very low incidence in primary GBM (3%–16%) and in pediatric GBM (0%–7%). In this context, we noted that, for 3 of our aggressive LGAs, transformation to higher-grade astrocytoma was confirmed by biopsies performed at disease progression. No data were available for the remaining patients in this group.

If IDH1 mutations cause or correlate with citrate accumulation, one would expect studies that report the in vivo detection of citrate in adults with secondary GBM, grade II and III astrocytomas but not for primary GBM. There have been, to the best of our knowledge, no such reports. There are 3 possible explanations for the lack of detection of citrate in astrocytomas in adults. First, there might be no such correlation. Second, IDH1 mutations might not be

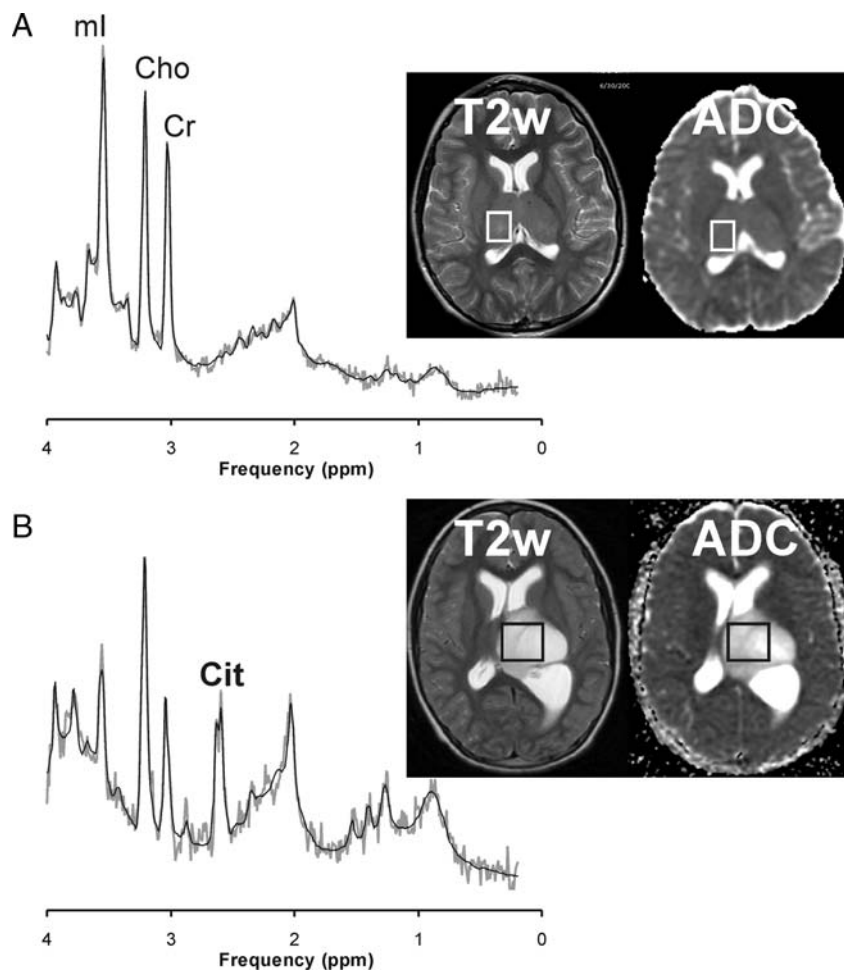


Fig. 4. No consistent pattern was observed for citrate (Cit) in grade III anaplastic astrocytoma. For example, there was no evidence of Cit in a patient with an anaplastic astrocytoma and gliomatosis cerebri (A). In contrast, in another patient with a hypocellular left thalamic anaplastic astrocytoma with intraventricular extension, Cit was readily detectable (B). Both spectra were acquired at initial presentation. Shown are also the apparent diffusion coefficient (ADC) maps for each patient. For the correlation with Cit concentrations, the mean ADC values were obtained from the area of the tumor that was also selected for the magnetic resonance spectroscopy (MRS) study. Cho indicates choline; Cr indicates creatine; ml indicates myo-inositol.

sufficient to cause citrate accumulation in adults with astrocytoma. Other mechanisms, such as increased activity of ATP citrate lyase,<sup>33</sup> the enzyme that breaks down cytosolic citric, could compensate for any effect IDH1 mutations might have on citrate levels. Third, citrate might have been overlooked in previous MRS studies, because its detection is technically demanding and investigators have not looked for citrate. It is noteworthy that, in a publication by Howe et al,<sup>16</sup> who used a similar short echo time single-voxel MRS approach as used in our studies, a figure shows peaks consistent with citrate for adult grade II and grade III astrocytoma, but not for GBM. Ultimately, studies that correlate IDH1 mutations with *in vivo* citrate levels are required to confirm a possible link.

The metabolism of tumors may also be altered due to physiological conditions. Increased interstitial fluid pressure (IFP) is a feature of many tumors and is an independent predictor of inferior outcomes, because it may prevent the uptake of macromolecular anti-cancer

agents.<sup>34–37</sup> However, the mechanism that would relate increased IFP and increased citrate is unclear. Another abnormal physiological condition postulated for tumors is hypoxia. Under hypoxic conditions, tumors increase glycolytic energy production and decrease mitochondrial function,<sup>38</sup> which may result in the observed accumulation of citrate. Hypoxic tumors have been associated with poor prognoses, because they show increased angiogenesis and local invasion, as well as increased formation of distant CNS metastases. They are more likely to transition to phenotypes that are more malignant. Hypoxic tumors are also considered more resistant to therapy.<sup>39–43</sup>

#### *Other Metabolic Features of Indolent LGA and Aggressive LGA*

NAA was also significantly differed between aggressive LGA and indolent LGA, albeit at a much lower level



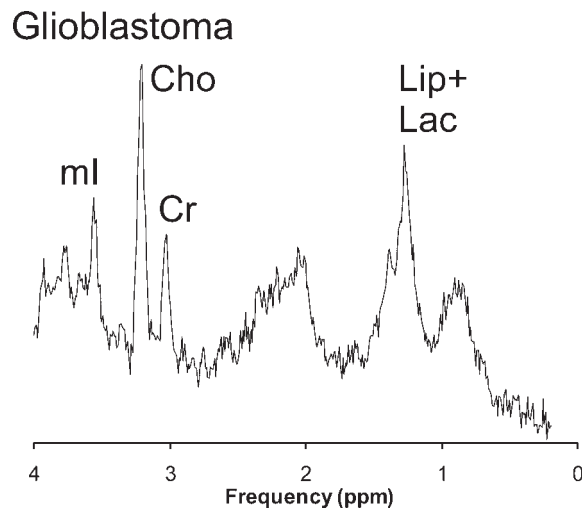


Fig. 5. Shown is a representative spectrum of biopsy-confirmed pediatric glioblastoma (average of three studies). Unlike for aggressive LGA and some anaplastic astrocytoma, there is no apparent citrate peak detectable at 2.6 ppm. Cho indicates choline; Cr indicates creatine; Lac indicates lactate; Lip indicates lipids; ml indicates myo-inositol.

than citrate. Because NAA is present in high concentrations only in normal neurons and axons,<sup>44,45</sup> low NAA in aggressive LGA likely indicated a small partial volume of normal tissue within those tumors. Among other chemicals detectable by MRS, choline, lactate, and lipids have been of particular interest in tumor spectroscopy. Choline-containing compounds are involved in cell membrane synthesis and breakdown and are abnormal in all forms of cancer.<sup>46,47</sup> Lactate is an indicator of abnormal glycolytic function, but it can also accumulate in necrotic tissue,<sup>13,48</sup> whereas lipid levels are believed to be elevated in aggressive, fast-growing tumors that are outgrowing their blood supply and causing necrosis in insufficiently perfused tumor tissue.<sup>49</sup> These metabolic features were not significantly different in aggressive LGA and indolent LGA in our study, which focused on magnetic resonance spectra acquired at an early stage of the disease. However, there is ample evidence in the literature that prominent choline, lactate, and lipids in spectra are indicators for malignant tumors.<sup>43,17,50</sup> In our study, these quantities progressively increased in aggressive LGA, when serial studies were available (cf. Fig. 3) consistent with what has been observed in previous publications,<sup>15–18,50–56</sup> whereas no significant changes were observed for indolent LGA. These measures are valuable for monitoring disease status, because they can often detect progression prior to clinical or radiological progression.<sup>15,51,52</sup>

#### Limitations

The number of patients included in this study was small. In addition, data were retrospectively evaluated, so there

is a higher risk of introducing a patient selection bias, although efforts were made to minimize this effect. Single-voxel MRS was used because this methodology provided robust and good-quality spectra in a timely fashion. On the other hand, single-voxel MRS is less practical for assessment of the heterogeneity of lesions, planning of focal treatments (such as radiation or surgical resection), and identification of areas of response to therapy and disease progression. We have conducted a limited number of multi-voxel studies of large bi-thalamic low-grade astrocytomas (not reported in detail) and noted, consistent with the positive correlation of citrate levels with ADC, that citrate levels are higher in the more edematous-appearing parts (ie, high ADC) of the lesion. Although these preliminary observations cannot be generalized at this stage, this is nevertheless a clear indication of the possibility of sampling errors in individual patients.

## Conclusions

An outcome-based comparison of grade II astrocytomas revealed that lesions with aggressive behavior within 2 years after diagnosis had significantly higher levels of citrate than did stable tumors. Prominent citrate may be an early sensitive indicator for pediatric grade II astrocytomas destined for aggressive behavior and, thus, useful for noninvasive patient stratification. Citrate was not specific for poor outcome, because it was not detectable in a significant portion of the high-grade astrocytomas. Among high-grade astrocytomas, tumors with prominent citrate may constitute a metabolic subclass.

## Acknowledgments

We thank Helen Petropoulos for her valuable suggestions and help with the discussion. We also thank Barbara Britt, Julia Castro, Joyce Derrickson, Anna Evans, Albert Joseph, and Arabhi Nagasunder for assistance with patient recruitment and the review of medical records and manuscript preparation. We thank Jane Tavare for help with the statistical analyses.

*Conflict of interest statement.* None declared.

## Funding

Ian's Friends Foundation, Rudi Schulte Research Institute, Thrasher Research Fund, and National Childhood Cancer Foundation (U01 CA97452-02).

## References

- Seymour ZA, Panigrahy A, Finlay JL, Nelson MD, Jr, Blüml S. Citrate in pediatric CNS tumors? *AJNR Am J Neuroradiol.* 2008;29(5):1006–1011.
- Warburg O. On the origin of cancer cells. *Science.* 1956;123(3191):309–314.
- Busch H, Davis JR, Olle EW. Citrate accumulation in slices of transplantable tumors of the rat. *Cancer Res.* 1957;17(7):711–716.
- Vander Heiden M, Cantley L, Thompson C. Understanding the Warburg effect: the metabolic requirements of cell proliferation. *Science.* 2009;324(5930):1029–1033.
- Farmer JP, Montes JL, Freeman CR, Meagher-Villemure K, Bond MC, O’Gorman AM. Brainstem Gliomas. A 10-year institutional review. *Pediatr Neurosurg.* 2001;34(4):206–214.
- Freeman CR, Farmer JP. Pediatric brain stem gliomas: a review. *Int J Radiat Oncol Biol Phys.* 1998;40(2):265–271.
- Mandell LR, Kadota R, Freeman C, et al. There is no role for hyperfractionated radiotherapy in the management of children with newly diagnosed diffuse intrinsic brainstem tumors: results of a Pediatric Oncology Group phase III trial comparing conventional vs. hyperfractionated radiotherapy. *Int J Radiat Oncol Biol Phys.* 1999;43(5):959–964.
- Pan E, Prados M. Brainstem Gliomas. In: Gupta, N, Haas-Kogen, D, Banerjee, A, eds. *Pediatric CNS Tumors.* Vol 3. Berlin/Heidelberg/New York: Springer; 2004:49–61.
- Nelson MD, Jr, Soni D, Baram TZ. Necrosis in pontine gliomas: radiation induced or natural history? *Radiology.* 1994;191(1):279–282.
- Yoshimura J, Onda K, Tanaka R, Takahashi H. Clinicopathological study of diffuse type brainstem gliomas: analysis of 40 autopsy cases. *Neurol Med Chir. (Tokyo).* 2003;43(8):375–382; discussion 382.
- Hargrave D, Bartels U, Bouffet E. Diffuse brainstem glioma in children: critical review of clinical trials. *Lancet Oncol.* 2006;7(3):241–248.
- Therasse P, Arbuick SG, Eisenhauer EA, Wanders J, Kaplan RS, Rubinstein L, Verweij J, Van Glabbeke M, van Oosterom AT, Christian MC, Gwyther SG. New guidelines to evaluate the response to treatment in solid tumors. European Organization for Research and Treatment of Cancer, National Cancer Institute of the United States, National Cancer Institute of Canada. *J Natl Cancer Inst.* 2000;92(3):205–216.
- Panigrahy A, Krieger MD, Gonzalez-Gomez I, et al. Quantitative Short Echo Time 1H-MR Spectroscopy of Untreated Pediatric Brain Tumors: Preoperative Diagnosis and Characterization. *AJNR Am J Neuroradiol.* 2006;27(3):560–572.
- Kovanlikaya A, Panigrahy A, Krieger M, et al. Untreated pediatric primitive neuroectodermal tumor in vivo: quantitation of taurine with MR spectroscopy. *Radiology.* 2005;236(3):1020–1025.
- Panigrahy A, Nelson MD, Jr, Finlay JL, et al. Metabolism of diffuse intrinsic brainstem gliomas in children. *Neuro Oncol.* 2008;10(1):32–44.
- Howe FA, Barton SJ, Cudlip SA, et al. Metabolic profiles of human brain tumors using quantitative in vivo 1H magnetic resonance spectroscopy. *Magn Reson Med.* 2003;49(2):223–232.
- Negendank WG, Sauter R, Brown TR, et al. Proton magnetic resonance spectroscopy in patients with glial tumors: a multicenter study. *J Neurosurg.* 1996;84(3):449–458.
- Stadlbauer A, Gruber S, Nimsky C, et al. Preoperative grading of gliomas by using metabolite quantification with high-spatial-resolution proton MR spectroscopic imaging. *Radiology.* 2006;238(3):958–969.
- Brown WD, Gilles FH, Tavaré CJ, et al. Prognostic limitations of the Daumas-Duport grading scheme in childhood supratentorial astroglial tumors. *J Neuropathol Exp Neurol.* 1998;57(11):1035–1040.
- Gilles FH, Brown WD, Leviton A, et al. Limitations of the World Health Organization classification of childhood supratentorial astrocytic tumors. Children Brain Tumor Consortium. *Cancer.* 2000;88(6):1477–1483.
- Reitman Z, Yan H. Isocitrate dehydrogenase 1 and 2 mutations in cancer: alterations at a crossroads of cellular metabolism. *J Natl Cancer Inst.* 2010;102(13):932–941.
- Gilles F, Tavaré C, Leviton A, et al. Prognostic limitations of the Daumas-Duport grading scheme in infratentorial neuroglial tumors in children. *Pediatr Dev Pathol.* 2004;7(2):138–147.
- Yan H, Bigner D, Velculescu V, Parsons D. Mutant metabolic enzymes are at the origin of gliomas. *Cancer Res.* 2009;69(24):9157–9159.
- Dóczi T, Schwarcz A. Correlation of apparent diffusion coefficient and computed tomography density in acute ischemic stroke. *Stroke.* 2003;34(5):e17–e18; author reply e17–e18.
- Murakami R, Sugahara T, Nakamura H, et al. Malignant supratentorial astrocytoma treated with postoperative radiation therapy: prognostic value of pretreatment quantitative diffusion-weighted MR imaging. *Radiology.* 2007;243(2):493–499.
- Higano S, Yun X, Kumabe T, et al. Malignant astrocytic tumors: clinical importance of apparent diffusion coefficient in prediction of grade and prognosis. *Radiology.* 2006;241(3):839–846.
- Chen HJ, Panigrahy A, Dhall G, Finlay JL, Nelson MD, Blüml S. Apparent diffusion and fractional anisotropy of diffuse intrinsic brain stem gliomas. *AJNR Am J Neuroradiol.* 2010;31(10):1879–1885.
- Parsons D, Jones S, Zhang X, et al. An integrated genomic analysis of human glioblastoma multiforme. *Science.* 2008;321(5897):1807–1812.
- Watanabe T, Nobusawa S, Kleihues P, Ohgaki H. IDH1 mutations are early events in the development of astrocytomas and oligodendrogliomas. *Am J Pathol.* 2009;174(4):1149–1153.
- Zhao S, Lin Y, Xu W, et al. Glioma-derived mutations in IDH1 dominantly inhibit IDH1 catalytic activity and induce HIF-1 $\alpha$ . *Science.* 2009;324(5924):261–265.
- Yan H, Parsons D, Jin G, et al. IDH1 and IDH2 mutations in gliomas. *N Engl J Med.* 2009;360(8):765–773.
- Dang L, White D, Gross S, et al. Cancer-associated IDH1 mutations produce 2-hydroxyglutarate. *Nature.* 2010;465(7300):966.
- Beckner M, Fellows-Mayle W, Zhang Z, et al. Identification of ATP citrate lyase as a positive regulator of glycolytic function in glioblastomas. *Int J Cancer.* 2010;126(10):2282–2295.
- Denko N. Hypoxia, HIF1 and glucose metabolism in the solid tumour. *Nat Rev Cancer.* 2008;8(9):705–713.
- Milosevic M, Fyles A, Hedley D, Hill R. The human tumor microenvironment: invasive (needle) measurement of oxygen and interstitial fluid pressure. *Semin Radiat Oncol.* 2004;14(3):249–258.
- Jain R, Baxter L. Mechanisms of heterogeneous distribution of monoclonal antibodies and other macromolecules in tumors: significance of elevated interstitial pressure. *Cancer Res.* 1988;48(24 Pt 1):7022–7032.
- Tong R, Boucher Y, Kozin S, Winkler F, Hicklin D, Jain R. Vascular normalization by vascular endothelial growth factor receptor 2 blockade induces a pressure gradient across the vasculature and improves drug penetration in tumors. *Cancer Res.* 2004;64(11):3731–3736.
- Höckel M, Vaupel P. Tumor hypoxia: definitions and current clinical, biologic, and molecular aspects. *J Natl Cancer Inst.* 2001;93(4):266–276.

39. Hockel M, Schlenger K, Aral B, Mitze M, Schaffer U, Vaupel P. Association between tumor hypoxia and malignant progression in advanced cancer of the uterine cervix. *Cancer Res.* 1996;56(19):4509–4515.
40. Hockel M, Schlenger K, Mitze M, Schaffer U, Vaupel P. Hypoxia and Radiation Response in Human Tumors. *Semin Radiat Oncol.* 1996;6(1):3–9.
41. Sutherland RM, Ausserer WA, Murphy BJ, Laderoute KR. Tumor Hypoxia and Heterogeneity: Challenges and Opportunities for the Future. *Semin Radiat Oncol.* 1996;6(1):59–70.
42. Jain RK, di Tomaso E, Duda DG, Loeffler JS, Sorensen AG, Batchelor TT. Angiogenesis in brain tumours. *Nat Rev Neurosci.* 2007;8(8):610–622.
43. Winkler F, Kozin SV, Tong RT, et al. Kinetics of vascular normalization by VEGFR2 blockade governs brain tumor response to radiation: role of oxygenation, angiopoietin-1, and matrix metalloproteinases. *Cancer Cell.* 2004;6(6):553–563.
44. Baslow MH. Canavan's spongiform leukodystrophy: a clinical anatomy of a genetic metabolic CNS disease. *Journal of Molecular Neuroscience.* 2000;15(2):61–69.
45. Tallan HH. Studies on the distribution of N-acetyl-L-aspartic acid in brain. *J Biol Chem.* 1957;224(1):41–45.
46. Ackerstaff E, Glunde K, Bhujwalla ZM. Choline phospholipid metabolism: a target in cancer cells? *J Cell Biochem.* 2003;90(3):525–533.
47. Podo F. Tumour phospholipid metabolism. *NMR Biomed.* 1999;12(7):413–439.
48. Hwang JH, Egnaczyk GF, Ballard E, Dunn RS, Holland SK, Ball WS, Jr. Proton MR spectroscopic characteristics of pediatric pilocytic astrocytomas. *AJNR Am J Neuroradiol.* 1998;19(3):535–540.
49. Negendank W, Sauter R. Intratumoral lipids in <sup>1</sup>H MRS in vivo in brain tumors: experience of the Siemens cooperative clinical trial. *Anticancer Res.* 1996;16(3B):1533–1538.
50. Negendank WG. Studies of human tumors by MRS: a review. *NMR in Biomedicine.* 1992;5:303–324.
51. Thakur SB, Karimi S, Dunkel IJ, Koutcher JA, Huang W. Longitudinal MR Spectroscopic Imaging of Pediatric Diffuse Pontine Tumors to Assess Tumor Aggression and Progression. *AJNR Am J Neuroradiol.* 2006;27(4):806–809.
52. Laprie A, Pirzkall A, Haas-Kogan DA, et al. Longitudinal multivoxel MR spectroscopy study of pediatric diffuse brainstem gliomas treated with radiotherapy. *Int J Radiat Oncol Biol Phys.* 2005;62(1):20–31.
53. Li BS, Wang H, Gonen O. Metabolite ratios to assumed stable creatine level may confound the quantification of proton brain MR spectroscopy. *Magn Reson Imaging.* 2003;21(8):923–928.
54. Shimizu H, Kumabe T, Shirane R, Yoshimoto T. Correlation between choline level measured by proton MR spectroscopy and Ki-67 labeling index in gliomas. *AJNR Am J Neuroradiol.* 2000;21(4):659–665.
55. Tamiya T, Kinoshita K, Ono Y, Matsumoto K, Furuta T, Ohmoto T. Proton magnetic resonance spectroscopy reflects cellular proliferative activity in astrocytomas. *Neuroradiology.* 2000;42(5):333–338.
56. Tedeschi G, Lundbom N, Raman R, et al. Increased choline signal coinciding with malignant degeneration of cerebral gliomas: a serial proton magnetic resonance spectroscopy imaging study. *J Neurosurg.* 1997;87(4):516–524.